GEOPHYSICAL RESEARCH LETTERS, VOL. 37, L14401, doi:10.1029/2010GL043967, 2010

The rainfall-no rainfall transition in a coupled land-convective atmosphere system

Alexandra G. Konings,[1] Gabriel G. Katul,[1,2] and Amilcare Porporato[1,2]

Received 13 May 2010; revised 8 June 2010; accepted 22 June 2010; published 27 July 2010.

[1] A one-dimensional representation of the atmospheric boundary layer (ABL) depth is coupled to a soil moisture bucket model to dynamically explore the relative roles of surface and free atmospheric conditions on convective precipitation occurrence and resulting soil moisture states. This occurrence is taken to depend on the crossing of the ABL height and the lifting condensation level in the presence of pure convective instability. If rainfall occurs (unrealistically) whenever these conditions are met, and free atmospheric conditions are constant, the resulting system state evolves towards a limit cycle with precipitation every day or every few days, or to a completely dry state. The free atmospheric humidity profile has a larger effect on determining the stationary soil moisture state than the temperature profile. The effect of dry air entrainment on surface energy partitioning decreases soil moisture sensitivity to free atmospheric conditions. **Citation:** Konings, A. G., G. G. Katul, and A. Porporato (2010), The rainfall-no rainfall transition in a coupled land-convective atmosphere system, *Geophys. Res. Lett.*, *37*, L14401, doi:10.1029/2010GL043967.

1. Introduction

[2] If atmospheric conditions are favorable, the soil moisture state may affect the disposition to and occurrence of convective rainfall [*Ek and Holtslag*, 2004; *Findell and Eltahir*, 2003]. Since soil moisture depends on rainfall occurrence, rainfall represents a feedback pathway in the coupled soil-plant-atmosphere system.

[3] This "soil-moisture precipitation feedback" has received significant research attention given its role in the climate system. The physical mechanisms of this feedback are complicated by a large number of interacting processes occurring between the land surface and the atmospheric boundary layer (ABL) state.

[4] *Juang et al.* [2007] analyzed two "necessary but not sufficient" conditions for rainfall to occur: (i) the crossing of the boundary layer height (h) and the lifting condensation level (LCL), and (ii) an atmosphere that supports the continuation of convection once it is initiated. With regards to the first necessary condition, surface processes and free atmospheric (FA) temperature and humidity profiles affect both ABL growth and LCL evolution, and often in counteractive ways. For example, a large surface heating and a low evaporative fraction (EF, the ratio of evapotranspiration to available energy) leads to increased boundary layer growth, entrainment of dry air and subsequent decrease in atmospheric humidity. The decrease in atmospheric humidity leads to an increased driving force for evaporation, resulting in a decrease in surface heat flux at later times. This pathway is referred to here as the dry-air entrainment feedback [*Santanello et al.*, 2007; *van Heerwaarden et al.*, 2009]. The initial increase in h promotes a crossing of the ABL and LCL; however, the subsequent reduction in atmospheric humidity elevates the LCL, making a crossing less likely.

[5] Given such simultaneous effects of surface and FA conditions on ABL and LCL dynamics, it is not surprising that much of the existing literature on the soil-moisture precipitation feedback generally falls into one of two categories: either the focus is on the effect of the land surface state under prescribed FA conditions tied to particular geographic locations [e.g., *Koster et al.*, 2006], or the effect of FA profiles on ABL and LCL dynamics given a land surface state [e.g., *Wu et al.*, 2009].

[6] The main objective here is to assess the relative importance of FA and surface conditions on the ABL's ability to support convective rainfall when both interact through the ABL. To do so, one must account not only for the auto-correlative properties of the FA parameters, but also the behavior of wind speeds and non-convective rain. Such an analysis would be prohibitively complex, preventing a clear theoretical treatment. Instead, this work explores the dynamics of an idealized coupled land surface-ABL system. Model results illustrate the preferential behavior of this coupled system, and clarify the role of land surface feedbacks.

2. Model Description

[7] A fully mixed ABL with potential temperature θ and specific humidity q constant throughout is assumed. The capping inversion at the top of the ABL is represented by an instantaneous jump in both variables. Such zeroth-order jump models are shown to be effective at describing primarily the evolution of the boundary layer states [*Pino et al.*, 2006]. Warm, dry air is entrained at the inversion. Heat and moisture are added to the boundary layer at the surface, as determined by a surface energy partitioning model that accounts for the effects of both the soil and ABL states. Here, convection can be triggered only when the ABL height and the LCL cross. When rainfall occurs, its depth depends on the atmospheric humidity profile. Figure 1 summarizes these modeled processes. The auxiliary material also summarizes the model equations and parameters.[3]

[1]Nicholas School of the Environment and Earth Sciences, Duke University, Durham, North Carolina, USA.
[2]Department of Civil and Environmental Engineering, Duke University, Durham, North Carolina, USA.

0094-8276/10/2010GL043967

[3]Auxiliary materials are available in the HTML. doi:10.1029/2010GL043967.

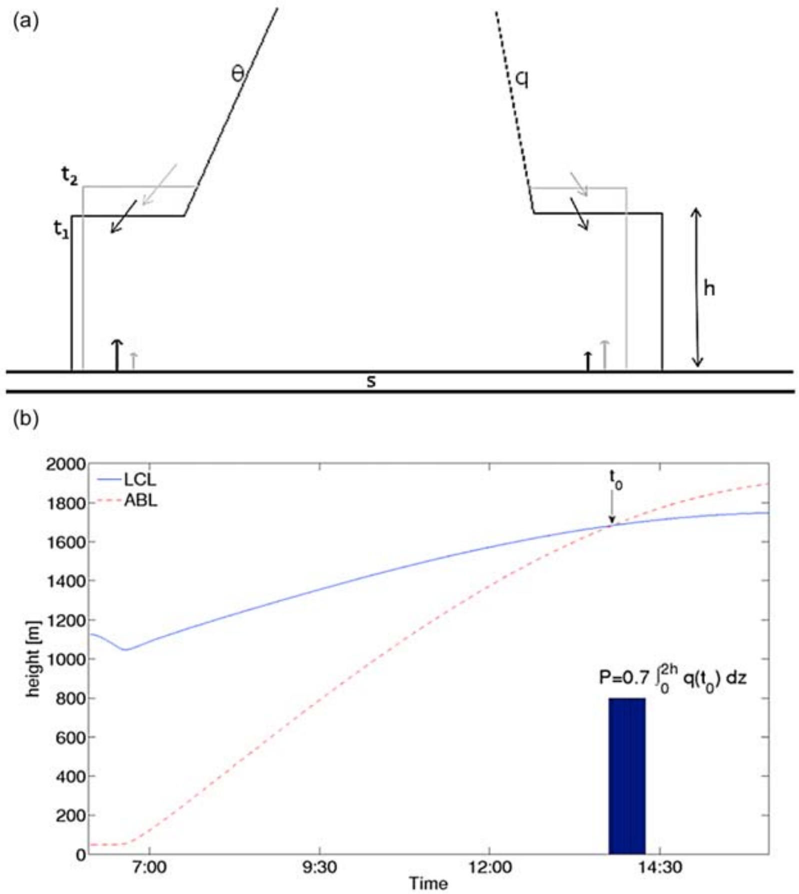

Figure 1. Summary of the modeled process. (a) Evolution of the ABL at each timestep and (b) rainfall "triggering".

[8] Heat and moisture fluxes at the surface are determined using an energy balance combined with the Penman-Monteith equation for evapotranspiration. Within the energy balance, net radiation R_n is determined using astronomical equations for shortwave radiation and the ground heat flux is assumed to be 15% of this R_n. Although the exact value of incoming radiation depends on latitude and time-of-year, these factors are not explicitly considered here. Instead, we scale R_n by a factor $R_n^{\max}$. The stomatal conductance g_s used in the Penman-Monteith equation is modeled according to a multiplicative Jarvis model, i.e., using stress functions of several factors to modify the maximum stomatal conductance $g_{\max}$. The g_s depends hyperbolically on the incident sunlight S (here proportional to R_n) [*Lhomme*, 2001]. It is also affected logarithmically by the vapor pressure deficit *VPD* [*Oren et al.*, 1999] and quadratically by θ [*Lhomme*, 2001]. Lastly, g_s depends on soil moisture s. If s is above a critical value s^*, $g_s = g_{\max}$, but g_s decreases linearly with s if below that value. If s is below the wilting point s_w, no evapotranspiration is possible [*Daly et al.*, 2004].

[9] The soil moisture in the root zone of depth Z_r is evolved using a simple bucket model. Drainage is given by a Darcian flux, assuming a unit gradient. Only a loamy soil is considered. The qualitative results in section 3 do not change for different soil types. Soil moisture is the only variable in the model with explicit day-to-day memory.

[10] The growth rate of the ABL is modeled using common 1-D energy balance considerations as by *Porporato* [2009] so that it is proportional to the surface heat flux $\overline{\theta' \omega'}_s$ and inversely proportional to γ_θ, the lapse rate above the boundary layer. Since convective rainfall generally does not occur at night, the evening collapse of the ABL is not explicitly considered. Instead, h is re-initialized to 50 m every morning.

[11] The FA θ and q profiles are modeled linearly with height z above the surface with slope γ and intercept ϕ, such that $\theta_o(z) = \gamma_\theta z + \phi_\theta$ and $q_o = \gamma_q z + \phi_q$. Simple conservation equations can then be used to determine the evolution of the mixed layer temperature and humidity.

[12] Daily early-morning sounding data from Greensboro, NC and Topeka, KS are used to estimate plausible FA profiles. The data set covers 36 years from May to September, when convective rainfall is most common. The lapse rate and intercept for both θ and q were estimated using a linear regression analysis applied between $z \in [300, 5000]$ m. Modelled θ and q are initialized every morning based on the profile intercepts. Early morning values depend on the residual layer remaining from the previous day's collapsed ABL. Since FA properties have finite autocorrelation, a relationship between early morning θ and q and their daily free atmospheric profiles is reasonable. The equivalence assumed is supported when comparing Greensboro sounding data with θ and q measurements taken at sunrise with an eddy-covariance tower 79 kilometers away at the Duke Forest near Durham, NC, described by *Juang et al.* [2007] (see the auxiliary material). Sounding data from

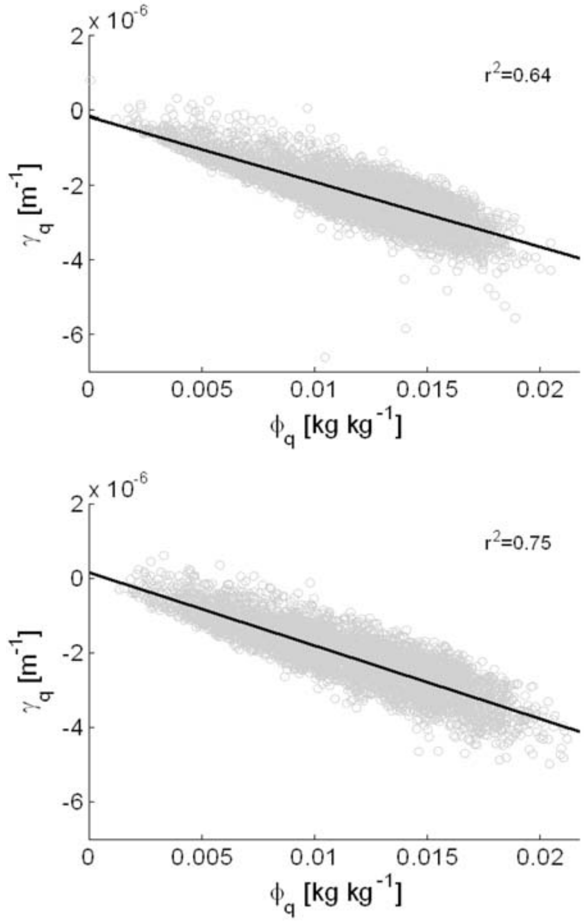

Figure 2. Scatter plot of daily free atmospheric humidity profile slope γ_q versus humidity profile intercept ϕ_q at (top) Greensboro, NC and (bottom) Topeka, KS.

both sites also support a negative linear relation between daily γ_q and ϕ_q, as shown in Figure 2. To reduce dimensionality, a similar relationship is adopted here. Although the exact relationship varies by location, qualitative results are not affected. In this case, $\gamma_q = -2.5 \times 10^{-4}\ \phi_q + 4 \times 10^{-7}\ m^{-1}$. Since the absolute value of the ABL θ (as influenced by ϕ_θ) has a far smaller effect than the absolute humidity, ϕ_θ is assumed constant at 294 K.

[13] Modeling the initiation and sustaining of convection is quite complex and well beyond the scope here. One possible simplification is requiring $-z/L > 5$, where L is the Obukhov length based on land-surface fluxes of momentum, heat and water vapor, and $z = h/2$. This atmospheric stability threshold of 5 was chosen because buoyant production of turbulent kinetic energy becomes dominant within the ABL [*Kader and Yaglom*, 1990], thereby ensuring the generation of convection with sufficient buoyant plume velocity to reach the level of free convection. *Juang et al.* [2007] used half-hourly eddy-covariance measurements and a boundary layer model to predict when these two conditions were met above a forested system near Durham, NC. They showed that these conditions can be used effectively to predict the timing of convective rainfall when it occurs. The same framework is used here.

[14] Since advection of water vapor is neglected, rainfall depth is taken to depend only on columnar water vapor [*Muller et al.*, 2009]. To prevent undue sensitivity to the height of the humidity profile, this column is "capped" at 2 h. The total water vapor is multiplied by a precipitation efficiency equal to 0.7 [*Brubaker and Entekhabi*, 1995]. The results in section 3 are not sensitive to the exact rainfall scheme used (except for very small depths, <1–2 mm). The soil moisture-rainfall feedback is primarily dependent on the occurrence of rainfall rather than its depth, in agreement with the results of *D'Odorico and Porporato* [2004].

3. Limiting Behavior

[15] To explore the limiting behavior of the model, we invoke two idealized assumptions: FA parameters are constant from day to day and precipitation always occurs when the triggering conditions are met. Depending on the combination of FA temperature and humidity profiles, the resulting stationary state for this simplified system is one of: rain storms occurring every day with oscillatory soil moisture behavior, a limit cycle in which rain storms occur every few days, or a permanent lack of rainfall. The final rainy/non-rainy state partly depends on the initial conditions for some combinations of FA parameters. The system evolves to the same stationary state independent of initial conditions when the initial $s > s^*$.

[16] The distribution of limiting behaviors is shown in Figure 3 for combinations of the maximum net radiation and of $g_{\max}$. As γ_θ decreases and h grows faster, rain is possible over a wider range of humidity conditions. For a given temperature profile, rain only occurs if ϕ_q is sufficiently high (or, due to the relationship between ϕ_q and γ_q used here, if γ_q is sufficiently low) so that the LCL is sufficiently low for a crossing. Based on Figure 3, the atmosphere's ability to support convective rainfall is more sensitive to the FA humidity profile than to the temperature profile. The former plays a stronger inhibitive role - when conditions are sufficiently dry, even the most unstable free atmospheres cannot support convection. Even for very stable free atmospheres, however, a sufficiently wet boundary layer still leads to triggering. Note that because of our assumption relating the early-morning humidity to ϕ_q and ϕ_q to γ_q, the sensitivity to γ_q shown in Figure 3 also occurs partially due to the influence of ϕ_q.

[17] An increase in R_n often leads to an increase in H, E, or both. The increase in H acts to increase h, while the increase in E tends to decrease the LCL (by increasing q). Therefore, precipitation is possible in a wider range of FA conditions, as shown in Figure 3. Because atmospheric humidity is less sensitive to direct changes in E than to changes in entrainment [*Juang et al.*, 2007; *Siqueira et al.*, 2009; *van Heerwaarden et al.*, 2009], the increase in h dominates. Thus, an increase in R_n generally leads convection to be triggered at a greater h. If only the EF is changed, however, the LCL is more responsive than h. As a result, increasing the EF through an increase in g_{max} (such as might occur due to changes in canopy height, leaf area index, or land use) increases the conditions under which the stationary state includes rain (Figure 3).

[18] Soil moisture limit cycles with period exceeding one day occur for only a limited region of parameter space (<5% of the plane in Figure 3). The period here refers to the number of days between rainfall events. In these cases, the minimum time between rain events is always greater than

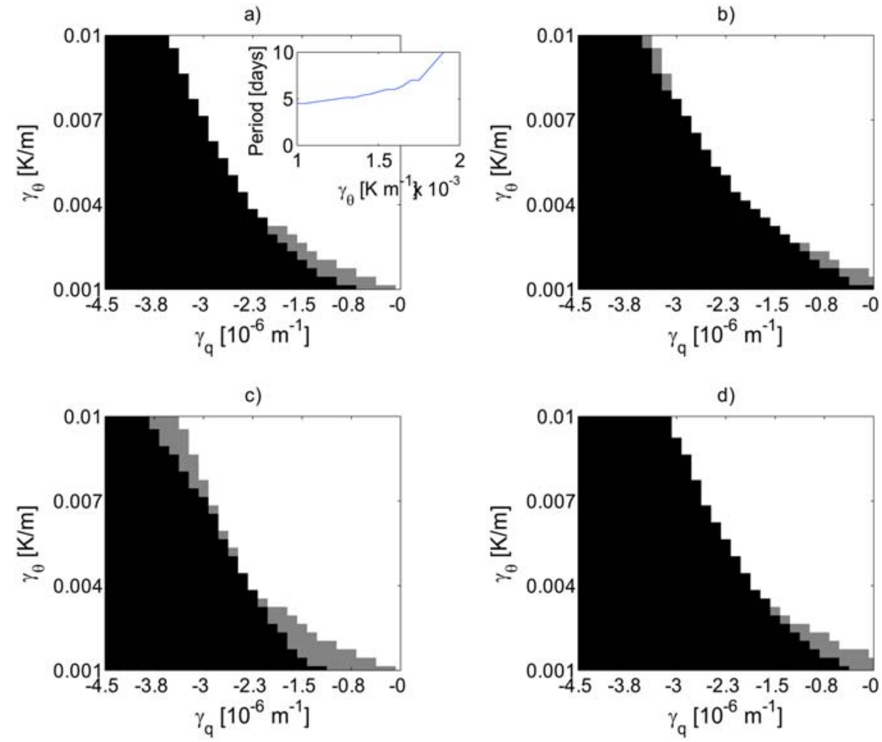

Figure 3. Stationary state space as a function of FA temperature and humidity profiles. Black indicates limit cycle with daily rainfall, gray indicates a limit cycle with a period greater than one day, and white areas do not rain. Each subplot represents a combination of daily $R_n^{\max}$ and $g_{\max}$: (a) $R_n^{\max} = 350$ W m^{-2} and $g_{\max} = 0.008$ m s^{-1}, (b) $R_n^{\max} = 600$ W m^{-2} and $g_{\max} = 0.008$ m s^{-1}, (c) $R_n^{\max} = 350$ W m^{-2} and $g_{\max} = 0.0016$ m s^{-1}, and (d) $R_n^{\max} = 600$ W m^{-2} and $g_{\max} = 0.0016$ m s^{-1}. The inset shows the period of the limit cycle as a function of γ_θ in K m^{-1} for $\gamma_q = -1 \times 10^{-6}$ m^{-1}.

one day. A few days after a rainfall event, the atmospheres of these limit cycles still support a crossing of the ABL and the LCL despite the low surface heating. However, this low surface heating is not conducive to convection (i.e., the $-z/L > 5$ condition is not met). Rainfall events cannot occur until the soil becomes sufficiently dry, leading to large H and elevated h. For a given FA humidity profile, the limit cycle period increases quasi-parabolically with γ_θ, matching the rate of increase of afternoon h.

4. Dry Air Entrainment Influence on Surface Partitioning

[19] The dry air entrainment feedback mentioned in the introduction significantly affects the shape of the rain-no rain boundary in Figure 3. If it is shut off (i.e., *VPD* is held at its early morning value when determining surface energy partitioning), sensitivity of precipitation occurrence to atmospheric humidity increases. The "boundary line" between rainy and dry conditions becomes even steeper. Figure 4 illustrates why, showing the mean daily EF as a function of s for various combinations of end members for FA temperature and humidity profiles. If entrainment does not affect surface energy partitioning, the EF is far less dependent on FA humidity than on FA temperature conditions. The dry air entrainment feedback, included in the curves in Figure 4 (bottom), increases EF through the increase of *VPD* over the course of the day. Due to the direct influence of FA humidity on the amount of entrainment, the resultant EF is also more dependent on FA humidity than on FA temperature conditions. Thus, the dry air entrainment feedback makes the rain/no-rain state less dependent on the FA humidity profile by allowing surface partitioning to partially compensate for changes in this profile.

[20] Figure 4 also illustrates why the stationary state is insensitive to initial soil moisture conditions only for sufficiently high s. The EF curve is steep near the wilting point. If s starts near this point, the LCL remains elevated throughout the day and rain is only possible under the most favorable conditions. As initial conditions move further away from the wilting point, the boundary line between rainy and non-rainy states moves closer to that shown in Figure 3. Nonetheless, soil moisture influences the possibility of rainfall only under a limited combination of FA parameters. Over only seven percent of the plane does a soil at s^* create a different rain/no-rain outcome than a soil at s_w.

5. Conclusions

[21] Using a coupled surface-ABL model and a simplified parametrization for rain occurrence, we can test the relative effect of surface energy partitioning and free atmospheric parameters on the soil moisture state with some tractability. For a given set of "permanent" FA parameters, the ecosystem always evolves towards either a completely dry state (desertification) or a limit cycle with daily or multi-day rainfall (wet-tropical). The transition between rainy and non-rainy states is a sharp function of FA parameters, and is more sensitive to the FA humidity profile than the FA

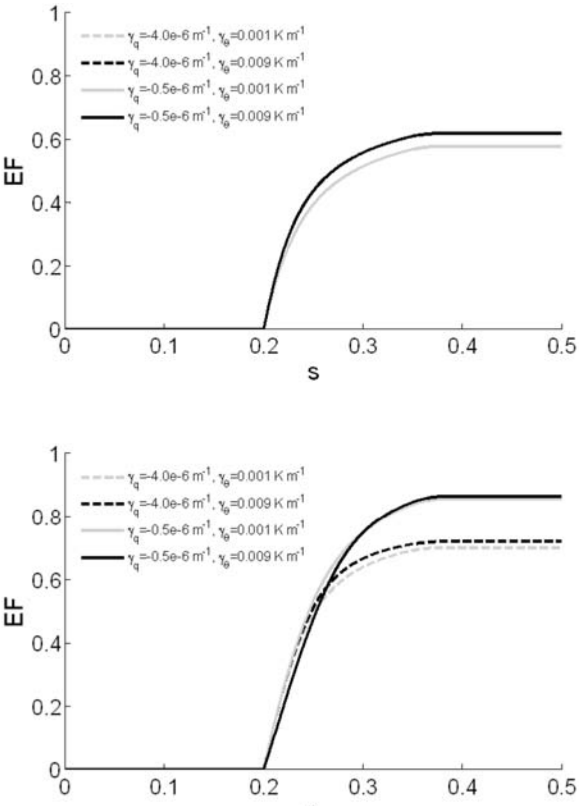

Figure 4. Daily mean evaporative fraction (EF) versus soil moisture (s) for various combinations of end-member profiles for FA θ and q. (top) Dry air entrainment feedback is artificially shut off by keeping *VPD* equal to its early-morning value when determining surface partitioning, and (bottom) dry air entrainment feedback is included. Rainfall occurrence is suppressed in both simulations. Note that dashed and solid lines overlap in Figure 4 (top).

temperature profile. The response of surface energy partitioning to dry air entrainment decreases sensitivity to the FA humidity profile. To resolve the effect of the free atmosphere on convective rainfall occurrence, it is necessary to account for both the rate of entrainment and the response of surface energy partitioning to the ABL state.

[22] Under more realistic temporally variable FA conditions, the occurrence statistics of convective rainfall and resulting soil moisture distribution are a function of the distributions of FA temperature and humidity profiles and their associated rain/no rain state. If those distributions are concentrated near the boundary between rainfall and non-rainfall supporting conditions, small changes in the boundary line (such as can be caused by changes in land surface conditions or seasonal changes in incoming radiation) may nevertheless have a large effect on the resulting potential for convective precipitation occurrence.

[23] **Acknowledgments.** A. G. Konings was supported by the National Science Foundation (NSF) through the Graduate Research Fellowship Program. Katul and Porporato acknowledge support from the NSF (NSF-EAR 0628342, NSF-EAR 0635787, NSF-ATM-0724088).

References

Brubaker, K. L., and D. Entekhabi (1995), An analytic approach to modeling land-atmosphere interaction: 1. Construct and equilibrium behavior, *Water Resour. Res.*, *31*(3), 619–632.

Daly, E., A. Porporato, and I. Rodriguez-Iturbe (2004), Coupled dynamics of photosynthesis, transpiration, and soil water balance. Part I: Upscaling from hourly to daily level, *J. Hydrometeorol.*, *5*(3), 546–558.

D'Odorico, P., and A. Porporato (2004), Preferential states in soil moisture and climate dynamics, *Proc. Natl. Acad. Sci. U. S. A.*, *101*(24), 8848–8851, doi:10.1073/pnas.0401428101.

Ek, M. B., and A. A. M. Holtslag (2004), Influence of soil moisture on boundary layer cloud development, *J. Hydrometeorol.*, *5*(1), 86–99.

Findell, K. L., and E. A. B. Eltahir (2003), Atmospheric controls on soil moisture-boundary layer interactions. Part I: Framework development, *J. Hydrometeorol.*, *4*(3), 552–569.

Juang, J.-Y., A. Porporato, P. C. Stoy, M. S. Siqueira, A. C. Oishi, M. Detto, H.-S. Kim, and G. G. Katul (2007), Hydrologic and atmospheric controls on initiation of convective precipitation events, *Water Resour. Res.*, *43*, W03421, doi:10.1029/2006WR004954.

Kader, B. A., and A. M. Yaglom (1990), Mean fields and fluctuation moments in unstably stratified turbulent boundary-layers, *J. Fluid Mech.*, *212*, 637–662.

Koster, R. D., et al. (2006), GLACE: The Global Land-Atmosphere Coupling Experiment. Part I: Overview, *J. Hydrometeorol.*, *7*(4), 590–610.

Lhomme, J. P. (2001), Stomatal control of transpiration: Examination of the Jarvis-type representation of canopy resistance in relation to humidity, *Water Resour. Res.*, *37*(3), 689–699.

Muller, C. J., L. E. Back, P. A. O'Gorman, and K. A. Emanuel (2009), A model for the relationship between tropical precipitation and column water vapor, *Geophys. Res. Lett.*, *36*, L16804, doi:10.1029/2009GL039667.

Oren, R., J. S. Sperry, G. G. Katul, D. E. Pataki, B. E. Ewers, N. Phillips, and K. V. R. Schafer (1999), Survey and synthesis of intra- and interspecific variation in stomatal sensitivity to vapour pressure deficit, *Plant Cell Environ.*, *22*(12), 1515–1526.

Pino, D., J. V. G. de Arellano, and S. W. Kim (2006), Representing sheared convective boundary layer by zeroth- and first-order-jump mixed-layer models: Large-eddy simulation verification, *J. Appl. Meteorol.*, *45*(9), 1224–1243.

Porporato, A. (2009), Atmospheric boundary-layer dynamics with constant Bowen ratio, *Boundary Layer Meteorol.*, *132*(2), 227–240, doi:10.1007/s10546-009-9400-8.

Santanello, J. A., M. A. Friedl, and M. B. Ek (2007), Convective planetary boundary layer interactions with the land surface at diurnal time scales: Diagnostics and feedbacks, *J. Hydrometeorol.*, *8*, 1082–1097, doi:10.1175/jhm614.1.

Siqueira, M., G. Katul, and A. Porporato (2009), Soil moisture feedbacks on convection triggers: The role of soil-plant hydrodynamics, *J. Hydrometeorol.*, *10*(1), 96–112, doi:10.1175/2008jhm1027.1.

van Heerwaarden, C. C., J. V. G. de Arellano, A. F. Moene, and A. A. M. Holtslag (2009), Interactions between dry-air entrainment, surface evaporation and convective boundary-layer development, *Q. J. R. Meteorol. Soc.*, *135*(642), 1277–1291, doi:10.1002/qj.431.

Wu, C. M., B. Stevens, and A. Arakawa (2009), What controls the transition from shallow to deep convection?, *J. Atmos. Sci.*, *66*(6), 1793–1806, doi:10.1175/2008jas2945.1.

G. G. Katul and A. G. Konings, Nicholas School of the Environment and Earth Sciences, Duke University, Box 90328, Durham, NC 27708, USA. (agk5@duke.edu)

A. Porporato, Department of Civil and Environmental Engineering, Duke University, Box 90287, 121 Hudson Hall, Durham, NC 27708, USA.